INTL JOURNAL OF ELECTRONICS AND TELECOMMUNICATIONS, 2018, VOL. 64, NO. 1, PP. 13–18
Manuscript received August 29, 2017; revised January, 2018. DOI: 10.24425/118140

Frequency Dependent Mismatch Correction Scheme for Zero-IF Receivers

Rafał Hibner and Ryszard J. Zieliński

***Abstract*—This paper shows effective method of linear distortions compensation in zero-IF receivers. With application of frequency domain processing a computation efficient method was developed that allows to correct quadrature mismatch in Zero-IF receiver along with gain and group delay independent of receiving signal type. Method was implemented and tested on hardware platform confirming its effectiveness. This method makes it possible to build high sensitivity devices to monitor spectrum in very wide frequency ranges.**

***Keywords*—Zero-if, ZIF, compensation, quadrature, IQ, wideband, dynamic range, image correction**

I. Introduction

ZERO-IF (ZIF) architecture plays dominant role in modern telecommunications systems. ZIF architecture is very compact and flexible solution that allows high integration. This architecture can be easily adjusted to new frequency band since most of filtering is performed in baseband. RF filter specifications are relaxed in comparison to heterodyne receiver. This caused wide adaptation of ZIF in commercial and military systems eg. communications, radar, ELectronic INTeligence (ELINT) etc. However, continuous growth of communications system capacity, higher orders of modulation and bandwidth rise the bar for receiving systems. Higher dynamic range is needed in order to meet those requirements. In ZIF receiver dynamic range is limited due to image response.

Due to imperfections during manufacturing process of components it is impossible to obtain signal in perfect quadrature. In a result perfect annihilation condition is not sustained within receiver. Any signal at the input will not only be observable at desired frequency, but also spurious image response will be observed on opposite sideband. In order to meet those growing needs correction mechanism need to be applied. Most methods are frequency independent and perform correction for single frequency [1] [2]. Those methods allow to obtain very high dynamic range but are band limited since mismatches vary with frequency. Many works focus on mismatch corrections in OFDM systems [3] [4] [5]. A few works incorporate frequency dependent corrections in generalized receiver systems [6] [9], which are indispensible in wideband systems. This work presents state of the art frequency dependent compensation scheme of quadrature mismatches (section II-A) that can be applied in any receiving system (independent of receiving signal type). The scheme is very computation efficient and also allows to correct other linear distortions with very few additional resources (section II-B and II-C). Section III describes hardware platform used to perform experiments.

Rafał Hibner is with SECOM Sp. z o.o., ul. Sernicka 21 50-503 Wrocław, Poland (e-mail: rafal.hibner@secom.com.pl).

Ryszard J. Zieliński is with Wrocław University of Science and Technology, ul. Wyspianskiego 27, 50-370 Wrocław, Poland (e-mail: ryszard.zielinski@pwr.edu.pl).

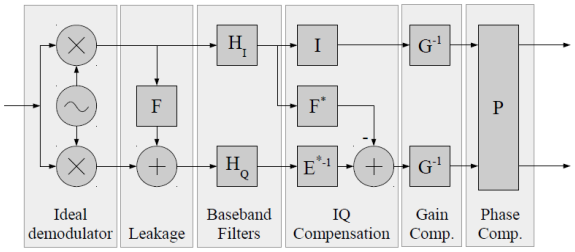

Fig. 1. Demodulator model with corrector.

II. Corrections

With all advantages of Zero-IF architecture there is hardware difficulty with achieving necessary phase and gain precision. Any mismatch in phase and/or gain results in reduced dynamic range due to spurious image signal. Such an effect is due to double mixer architecture. In ZIF receiver input signal is multiplied with local oscillator in I-branch and 90° phase shifted version of the same local oscillator in Q-branch (Fig. 1). The resulting signals represent real and imaginary parts of analytical signal describing down-converted version of input signal. Down-conversion is performed from local oscillators center frequency directly to baseband. Image response that usually appears during mixing process is annihilated since image response in I and Q branch is 180° shifted (after another 90° shift within DFT) with the same amplitude. However, in real implementations due to fabrication imperfections the I and Q responses are not in perfect quadrature and not equal in amplitude. In Fig. 2 can be seen IMage Rejection Ratio (IMRR) calculated using formula 1 as a function of phase error ϕ_e for different amplitude errors A_e. Those mismatches break perfect annihilation condition. As a result spurious signal appears (Fig. 4).

A. IQ correction

The magnitude of spurious signal is directly tied to input signal magnitude and the mismatches. Figure of merit describing this phenomenon is IMage Rejection Ratio (IMRR). This parameter describes magnitude ratio of existing input signal to false unannihilated image response. The IMRR can be mathematically tied to phase error ϕ_e and amplitude error A_e with formula 1 [8].

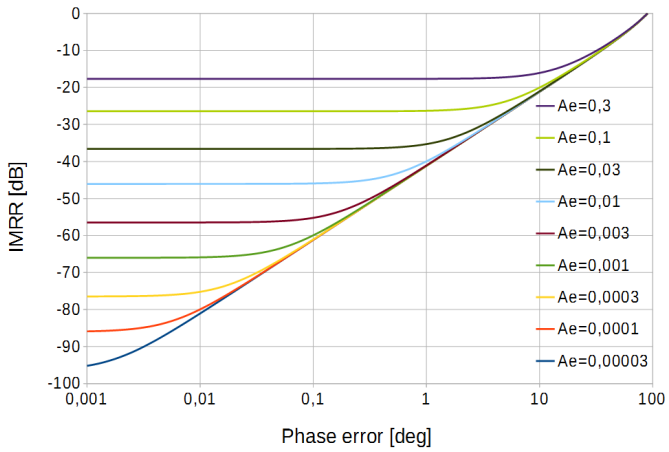

Fig. 2. Theoretical IMage Rejection Ratio.

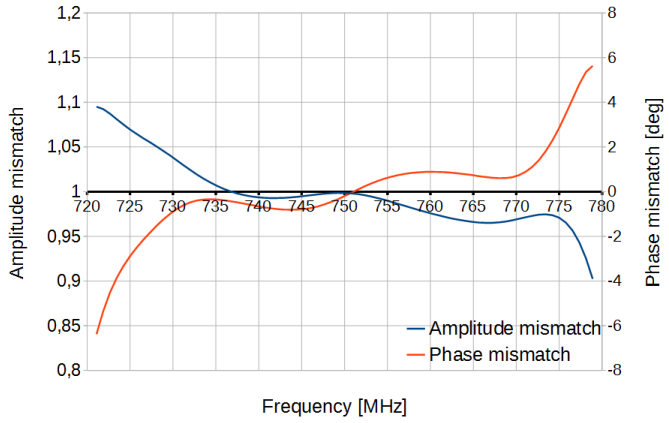

Fig. 3. Mismatch characteristic C(f).

$$IMRR = \frac{1 + 2 \cdot (1 + A_e) \cdot cos\phi_e + (1 + A_e)^2}{1 - 2 \cdot (1 + A_e) \cdot cos\phi_e + (1 + A_e)^2} \quad (1)$$

With careful hardware design and additional analog compensation IMRR of -40 to -50 dB is achievable [11]. That corresponds to phase error less than 1° and amplitude error less than 0.02 . Higher IMRR is not feasible because the analog compensation is only effective in narrow band. It is because of the fact that mismatches (amplitude and phase) are frequency dependent as was presented in Fig. 3. Due to this fact single point analog compensations can enhance IMRR only in narrow band region. Further enhancements are only possible with frequency dependent compensations.

There are several methods of IQ mismatch corrections. Some of them are data aided [7] while others use dedicated test signal generator [8]. Method involving test signal generator is used in this work.

The method is based on off-line mismatch estimation. The process of estimation requires simple Continuous Wave (CW) test signal and phase/amplitude estimator. With the test signal present at the input of demodulator phase shift between as well as amplitude mismatch between I and Q channels can be measured. In order to obtain characteristics that are easily

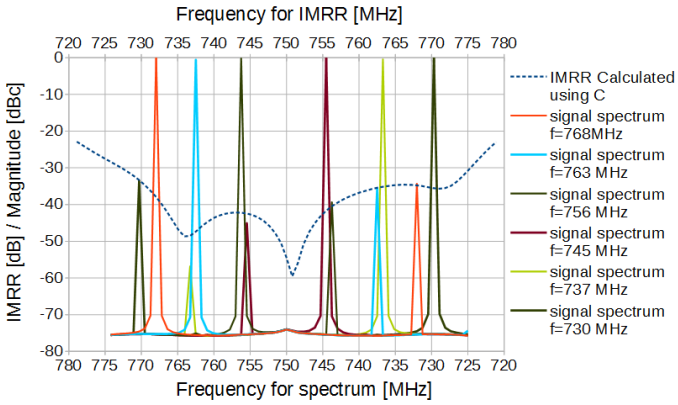

Fig. 4. Calculated IMRR with test signals depicting leakage.

applicable in compensations measurement is performed at center of every Discrete Fourier Transform frequency bin. In ideal case phase shift will be $-sgn(f) \cdot 90^\circ$ and amplitude ratio would be 1. With measurement performed on multiple frequency points within band we obtain characteristic C describing those mismatches (Fig. 3). Using equations 2 estimates for characteristics E^{*-1} and F^* can be calculated for measured C. $E = \frac{H_Q}{H_I}$ denotes differences in transfer functions between In-phase and Quadrature channels and F denotes leakage between channels (fig. 1).

Additionally using characteristic C we can calculate theoretical IMRR. Figure 4 presents calculated IMRR along with several CW signal spectra. Frequency axis for spectra was reversed around 750MHz in order to align image response with corresponding IMRR parameter value.

$$F^*(\omega) = -jsgn(\omega)\frac{C(\omega) + \overline{C(-\omega)}}{C(\omega) - \overline{C(-\omega)}}$$
$$E^{*-1}(\omega) = \frac{-2jsgn(\omega)}{C(\omega) - \overline{C(-\omega)}} \quad (2)$$

Overline denotes complex conjugate.

After obtaining mismatch characteristics compensation can be performed. The process involves applying inverse distortions to modeled ones. Figure 1 depicts demodulator with modeled mismatches along with compensation mechanism. Correction procedure involves applying inverse distortions to the measured ones. After IQ compensation procedure the signal should be in perfect quadrature with equal amplitude. The gain/phase characteristics for both I and Q paths is identical and correspond to H_I characteristic. Figure 5 presents signal spectra after corrections were applied. Image response is substantially reduced and clean reliable spectrum is obtained.

The main effort is to implement E^{*-1} and F^* frequency dependent transfer functions efficiently. The complexity of those transfer functions depends on required compensation precision (number of compensation frequency points). If we need higher IMRR we need to estimate and correct mismatches in finer frequency intervals.

The standard approach would be generation of FIR filters of impulse response given by inverse Discrete Fourier Transform

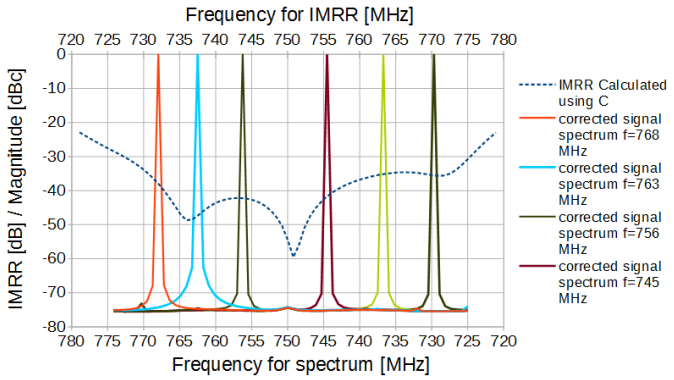

Fig. 5. Leakage after correction.

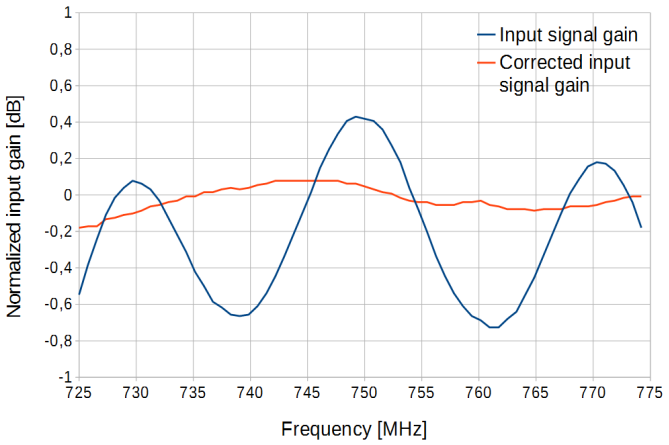

Fig. 6. Gain unevenness.

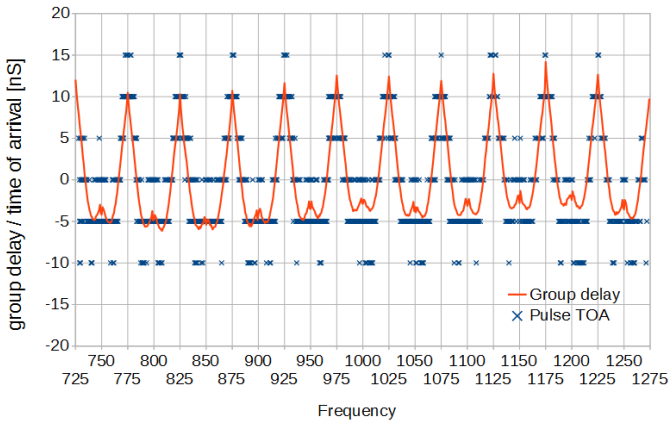

Fig. 7. Normalized measured group delay and pulse TOA discrepancy.

(DFT) of the transfer functions E^{*-1} and F^*. While being very easy and straightforward approach it is very resource consuming. Two asymmetric FIR filters of N^{th} order require $2N$ multipliers.

An alternative approach to implement desired filtration is to use frequency domain filtering. To do so we need to calculate DFT of In-phase and Quadrature path signals separately. Then implementation of F^* and E^{*-1} is equivalent to multiplying of those signals with complex correction coefficients for corresponding frequency. This solution, with the use of Fast Fourier Transform (FFT) algorithm reduces number of required multipliers to $2 \cdot 2 \cdot log_2 N + 2 \cdot 4$ instead of $2N$. The $log_2 N$ multipliers for each FFT (2 channels, forward and inverse transform) and 4 additional for each complex multiplier. This can be easily pushed even further if we exploit the fact that the M_{IF} and M_{QF} signals are real valued (although M_{QF} represents imaginary part of analytical signal the voltage itself is real valued). Therefore, we can use one FFT to calculate two real valued transforms [10]. Now only $2log_2 N + 8$ multipliers are needed. If N is greater or equal to 8 it becomes more efficient to use frequency domain approach. Furthermore, many applications need to calculate DFT anyways. In such a case only 8 additional multipliers are needed in design to implement corrections. The correction coefficients E^{*-1} F^* can be stored in lookup table where each row contains correction coefficients for different frequency (DFT bin).

B. Gain correction

To properly correct IQ mismatch the amplitude of test signal generator does not need to be precisely controlled. However, if the test signal generator has constant amplitude over band of interest additional gain compensation can be performed. During measurement of C characteristics signal level (denoted as G) is also intrinsically measured. Using this data we can compensate gain unevenness. Figure 6 presents gain unevenness before and after correction. Discrepancies after correction are due to uneven test signal generator power level. Similarly to quadrature compensation, if we use frequency domain approach, gain correction requires only 2 multipliers to change gain of I and Q channels. Additionally, if we precalculate E^{*-1} and F^* coefficients (correcting Q channel) to incorporate gain corrections only one additional multiplier is needed to correct I channel.

C. Phase/Group delay correction

The last linear distortion that can be compensated with few additional components is group delay/phase shift. Group delay T_g and phase shift ϕ are tightly coupled. Group delay is negated derivative of phase shift with respect to frequency (eq. 3).

$$T_g(\omega) = -\frac{d\phi(\omega)}{d\omega} \tag{3}$$

Therefore, in order to flatten group delay we need to linearize phase shift. To do so the phase characteristics has to be measured first. Direct measurement of phase shift is difficult. Fortunately, absolute value of phase shift is not needed. Only linearity of phase is important. Therefore, if we measure group delay $T_g^*(\omega)$ with constant error C_1 we can calculate phase shift to within arbitrary linear factor using formulas 4-6.

$$T_g^*(\omega) = T_g(\omega) + C_1 \tag{4}$$

$$\int T_g^*(\omega)d\omega = \int T_g(\omega)d\omega + C_1\omega \tag{5}$$

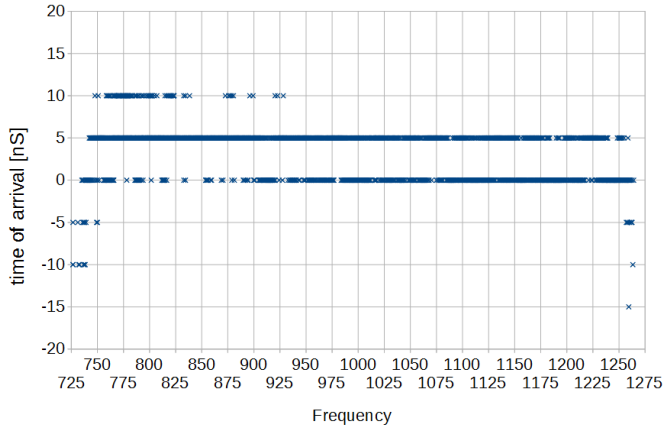

Fig. 8. Pulse TOA after phase/group delay compensation.

$$\int T_g^*(\omega)d\omega = \phi(\omega) + C_1\omega + C_2 \tag{6}$$

To measure group delay additional amplitude modulator for test signal generator is needed. Simplest On-Off-Keying (OOK) modulation is sufficient. Group delay can be measured (with constant error) as phase shift between modulating signal (envelope) and demodulated signal amplitude. The result of such a measurement for system consisting of 11 ZIF receivers is presented in Fig. 7. More in-depth description of system is in section III. Along with group delay pulse Time Of Arrival (TOA) measured by the system without group delay compensation is presented in the plot. Using measured data and formula 6, phase shift within the band was calculated. Based on that phase correction characteristics P was calculated in order to linearize it.

After correction was applied TOA precision was increased to within one sample - 5nS (fig. 8). Only discrepancies occurred at band edge where signal got significantly distorted due to band edge.

In a case where multiple receiver are use to increase receiver bandwidth it is also important to maintain phase continuity. Figure 9 represents normalized phase shift within receiver. The waveing of the plot is due to phase shift within receiver. However discontinuities are due to different phase of the local oscillators within receivers. Such discontinuities also need to be compensated for. Without it the received signal would be distorted.

Figure 10 shows pulse received by a channel with phase difference within the band. It is clear that uncontrolled phase shift due to inherent phased locked loop operation causes severe distortions in parallel channel topology.

The correction of such distortion is simple and can be incorporated within the correction of phase front. The measurement of the discontinuity can be made during estimation of C characteristic. Phase difference viewed by two adjacent channels receiving signal with test generator tuned on the boundary between those channels, corresponds to the phase discontinuity. This phase misalignment, due to its nature, are frequency independent. Therefore the correction mechanism need to incorporate one additional constant factor for each

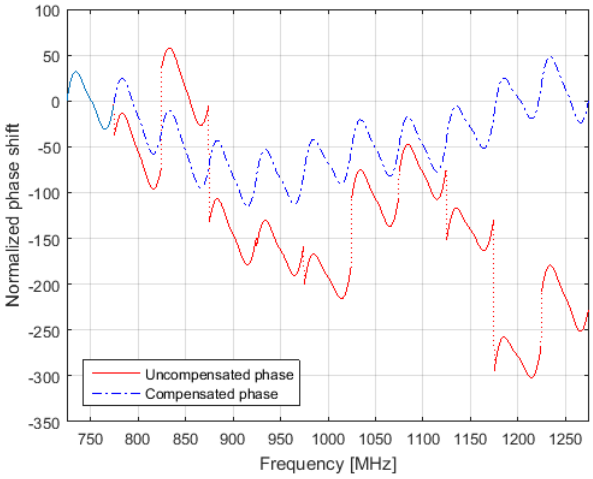

Fig. 9. Normalized phase shift with and without phase continuity compensation.

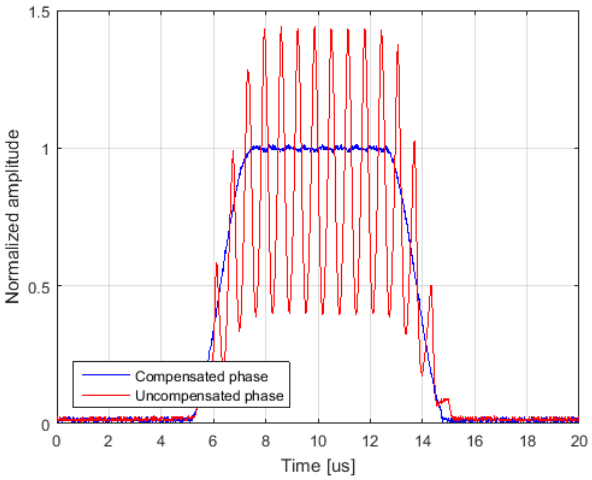

Fig. 10. Signal shape/distortion with and without phase continuity compensation.

channel. No additional resources are needed in addition to those used for group delay corrections.

D. Windowing

In many applications windowing of DFT is essential for proper operation. Described method does not allow for time domain windowing of DFT. Time domain multiplication of signal with window function causes frequency domain correlation of window spectrum with input signal spectrum. As a result we lose orthogonality and corrections are degraded. The obvious way around that is to calculate inverse Fourier transform and than calculate windowed Fourier transform. However there is a simpler more efficient way. Since time domain multiplication corresponds to frequency domain correlation we can correlate our corrected signal with window spectrum. The result will be the same and since most window functions have simple spectral representation the required FIR filter for correlation would need only few taps. For

TABLE I
CORRECTOR RESOURCE UTILIZATION

Luts	2638
Slice	1080
DSPs	37
Block RAM	8

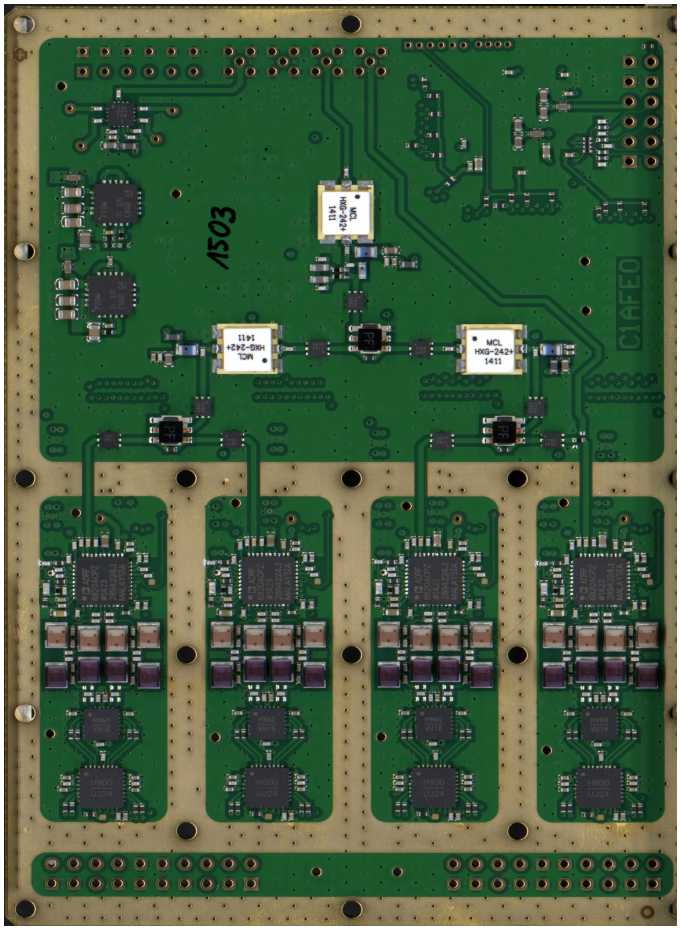

Fig. 11. Analog part of hardware platform used in experiments.

example Hamming window spectral representation has only 3 symmetric samples. Therefore, the windowing filter would require only 2 multipliers on real path and 2 on imaginary path regardless of FFT length.

III. EXPERIMENTAL PLATFORM

Figure 11 presents part of hardware platform used to carryout the experiments. There are 4 receiver channels implemented on a single board. Measurements were carried out on platform consisting of 11 ZIF channels (3 boards from fig. 11 working in synchronization) covering total bandwidth of 550MHz. Each channel used dual 14 bit ADC with analog bandwidth 60MHz sampling at 200MSps. All ZIF tuners had all above-mentioned corrections implemented. The estimation and compensation was performed on 256 evenly spaced frequency intervals (every 0.78125MHz) within each channel. Figures 3-6 show measurements carried out in one of the channels. Figures 7-8 show aggregated measurements of 11 channels. Signal processing was implemented in 7 series Xilinx FPGAs. Resources used for single channel corrections are presented in table I. The implemented correctors use only one FFT transform. Inverse transform is not incorporated in resource utilization. Achieved Spurious Free Dynamic Range (SFDR) exceeded 75dB. Linear distortions were not limiting the dynamic range. Additionally, gain unevenness was corrected to within test signal generator level stability. Group delay compensation enhanced TOA precision to within measurement resolution (5ns). With phase difference correction on channels boundary no distortions were observable. Additionally no significant degradation in time of receiver parameters running on constant correction parameters was observed, however device itself had temperature stabilization circuitry.

IV. SUMMARY

Presented scheme gives sufficient performance even for most demanding applications. With additional nonlinear corrections or better demodulator SFDR over 80dB should be easily achievable. All relevant linear distortions can be efficiently corrected. Frequency domain corrections are very computation efficient and are independent of received signal. Only additional component needed is test signal generator with simplest OOK modulator. This frequency domain compensation scheme can also be used in applications using time domain processing with the use of additional inverse Fourier transform. With growth of signal processing power in current FPGAs such corrections can easily be incorporated in any receiving system. Due to frequency domain processing filter synthesis is unnecessary. What is more, presented method is scalable. Number of correction points can be easily changed with little impact on needed resources. Requirements for additional multipliers grows logarithmically with correction points. The presented method is based on mismatch estimation before operation, however other means of mismatch estimation, like data aided, should be applicable. In test application test signal generator was incorporated in receiver and work both as test signal generator and Build In Test Equipment (for self testing purposes). However factory calibration should be sufficient in most midrange receivers.

REFERENCES

[1] Il-Hyun Sohn, Eui-Rim Jeong and Y. H. Lee, "Data-aided approach to I/Q mismatch and DC offset compensation in communication receivers," in IEEE Communications Letters, vol. 6, no. 12, pp. 547-549, Dec. 2002. doi: 10.1109/LCOMM.2002.806451

[2] H. Wang, Y. Lu, X. Wang and C. Wang, "Digital I/Q Imbalance Compensation in Quadrature Receivers," 2006 CIE International Conference on Radar, Shanghai, 2006, pp. 1-4. doi: 10.1109/ICR.2006.343527

[3] B. Narasimhan, D. Wang, S. Narayanan, H. Minn and N. Al-Dhahir, "Digital Compensation of Frequency-Dependent Joint Tx/Rx I/Q Imbalance in OFDM Systems Under High Mobility," in IEEE Journal of Selected Topics in Signal Processing, vol. 3, no. 3, pp. 405-417, June 2009. doi: 10.1109/JSTSP.2009.2020325

[4] B. Narasimhan, S. Narayanan, N. Al-Dhahir and H. Minn, "Digital baseband compensation of joint TX/RX frequency-dependent I/Q imbalance in mobile MIMO-OFDM transceivers," 2009 43rd Annual Conference on Information Sciences and Systems, Baltimore, MD, 2009, pp. 545-550. doi: 10.1109/CISS.2009.5054780

[5] Tubbax, Jan, et al. ”Compensation of IQ imbalance in OFDM systems.” Communications, 2003. ICC'03. IEEE International Conference on. Vol. 5. IEEE, 2003. doi: 10.1109/ICC.2003.1204086

[6] Kong-Pang Pun, J. E. Franca and C. Azeredo-Leme, ”Wideband digital correction of I and Q mismatch in quadrature radio receivers,” 2000 IEEE International Symposium on Circuits and Systems. Emerging Technologies for the 21st Century. Proceedings (IEEE Cat No.00CH36353), Geneva, 2000, pp. 661-664 vol.5. doi: 10.1109/ISCAS.2000.857556

[7] Chung, Yuan-Hwui, and See-May Phoong. ”Estimation of Frequency Selective I/Q Imbalance and CFO for OFDM Systems.” Proceedings: APSIPA ASC 2009: Asia-Pacific Signal and Information Processing Association, 2009 Annual Summit and Conference. Asia-Pacific Signal and Information Processing Association, 2009 Annual Summit and Conference, International Organizing Committee, 2009.

[8] G. Vallant, M. Epp, W. Schlecker, U. Schneider, L. Anttila, and M. Valkama, “Analog iq impairments in zero-if radar receivers: Analysis, measurements and digital compensation,” in *Instrumentation and Measurement Technology Conference (I2MTC), 2012 IEEE International*, pp. 1703–1707, 2012. doi: 10.1109/I2MTC.2012.6229222

[9] R. Hibner ”Adaptive I/Q mismatch correction” Master Thesis at Wrocaw University of Technology, 2013

[10] Robert Matusiak “Implementing Fast Fourier Transform Algorithms of Real-Valued Sequences With the TMS320 DSP Platform” Digital Signal Processing Solutions, Texas Instruments Application Report 2001 www.ti.com/lit/an/spra291/spra291.pdf

[11] Yinhao Ding and M. Trinkle, ”Dynamic range considerations for wideband Zero-IF receivers,” 2009 4th IEEE Conference on Industrial Electronics and Applications, Xi'an, 2009, pp. 1976-1981. doi: 10.1109/ICIEA.2009.5138548